Chemistry and Physics of Lipids 207 (2017) 38–48

Contents lists available at ScienceDirect

Chemistry and Physics of Lipids

journal homepage: www.elsevier.com/locate/chemphyslip

The insertion of Polybia-MP1 peptide into phospholipid monolayers is regulated by its anionic nature and phase state

Dayane S. Alvares[a], Natalia Wilke[b], João Ruggiero Neto[a,*], Maria Laura Fanani[b,*]

[a] UNESP – São Paulo State University, IBILCE, Department of Physics, São José do Rio Preto, SP, Brazil
[b] Centro de Investigaciones en Química Biológica de Córdoba (CIQUIBIC-CONICET), Departamento de Química Biológica, Facultas de Ciencias Químicas, Universidad Nacional de Córdoba, Argentina

ARTICLE INFO

Keywords:
Lipid domains
Brewster angle microscopy
Membrane penetration
Peptide adsorption
Antimicrobial peptide

ABSTRACT

Polybia-MP1 or simply MP1 (IDWKKLLDAAKQIL-NH_2) is a peptide with broad-spectrum bactericidal activity and a strong inhibitory effect against cancer cells. The aim of this work was to evaluate the effect of biophysical properties such as membrane texture and film thickness on MP1 interaction with neutral and anionic lipid membranes. For this purpose, we first explored the peptide's surface behavior. MP1 showed high surface activity, adsorbing onto bare air/aqueous interfaces up to higher surface pressures than the collapse pressure of MP1 Langmuir films. The MP1-lipid membrane interaction was studied using Langmuir phosphatidylcholine and phosphatidylserine (PS) monolayers as model membrane systems. PS was chosen since this negatively charged lipid was found predominantly on the outer leaflet of tumor cells, and it enhances MP1 activity for PS-containing membranes to a greater extent than for other negatively charged lipids. MP1 incorporated into anionic PS monolayers, which show a liquid-expanded (LE) phase or LE-liquid-condensed (LC) phase coexistence, up to lipid-packing densities higher than those of cell membranes. The mixed lipid/MP1 films were explored by Brewster angle microscopy and atomic force microscopy. MP1 partitioned preferentially into the LE phase state of PS films, and were thus excluded from the coexisting LC phase. This interaction had strong electrostatic bases: in pure water, the lipid-peptide interaction was strong enough to induce formation of reversible lipid-peptide 3D structures associated with the interface. MP1 incorporation into the LE phase was accompanied by a shift of the phase transition pressure to higher values and a thinning of the lipid film. These results showed a clear correlation between peptide penetration capacity and the presence or induction of the thin LE phase. This capacity to regulate membrane physical properties may be of relevance in the binding, incorporation and membrane selectivity of this promising antitumor peptide.

1. Introduction

Antimicrobial peptides form a large family of short sequence (< 50 amino acids) peptides, which usually display a cationic nature at physiological pH and exhibit amphiphilic helical structures when interacting with membranes. They interact directly with the lipid matrix of cell membranes and are highly selective for the anionic membrane surface, often disrupting lipid-packing and resulting in cell lysis (Bechinger, 2015). The amphipathic cationic peptide Polybia MP-1 (IDWKKLLDAAKQIL-NH_2), or simply MP1, is one example of these peptides. Extracted from the venom of the Brazilian wasp *Polybia paulista,* the peptide exhibits a broad-spectrum bactericidal activity without being hemolytic or cytotoxic (Souza et al., 2005). Recent studies have shown that this peptide also displayed an inhibitory effect on the proliferation of prostate and bladder cancer cells (Wang et al., 2008) and multidrug-resistant leukemic cells (Wang et al., 2009). Furthermore, it was observed that MP1 selectively recognized leukemic T-lymphocytes and not healthy ones (Dos Santos Cabrera et al., 2012).

Since this peptide acts only on the lipid matrix of the membrane without requiring membrane receptors, we expected that the membrane properties regulated by lipid composition, such as surface electrostatic and phase state, could be involved in this selective recognition. In healthy human cells, lipids are asymmetrically distributed in the outer and inner leaflets, and the aminophospholipid phosphatidylserine (PS) is most probably located in the inner leaflet of the plasma membrane (Devaux, 1992). In cancer cells, PS is externalized to the outer leaflet, resulting in an anionic membrane surface that could be a source for selective recognition by amphipathic cationic peptides (Bechinger, 2015; Fadok et al., 1998, 1992; Riedl et al., 2011; Utsugi et al., 1991).

The effect of PS on the lytic activity of MP1 was explored in giant

* Corresponding authors.
E-mail addresses: jruggiero@sjrp.unesp.br (J. Ruggiero Neto), lfanani@gmail.com (M.L. Fanani).

http://dx.doi.org/10.1016/j.chemphyslip.2017.08.001
Received 2 June 2017; Received in revised form 30 July 2017; Accepted 5 August 2017
Available online 10 August 2017

and large unilamellar vesicles. These studies provided valuable evidence that PS acts synergistically with phosphatidylethanolamine (PE) lipids (Bueno Leite et al., 2015) and liquid-ordered domains (composed of sphingomyelin and cholesterol) (Alvares et al., 2017) regulating the lytic efficiency of MP1. PS was shown to have important properties that contribute to the efficiency of MP1 in disturbing lipid-packing, leading to membrane destabilization, since replacing PS by other anionic lipids, such as phosphatidylglycerol and cardiolipin, did not result in enhanced lytic activity (Alvares et al., 2017; Dos Santos Cabrera et al., 2012). These findings show that PS may provide lipid membranes with features other than just a net negative surface charge, including the ability to regulate MP1 binding and action.

The phospholipid monolayer has been used for four decades as a model lipid membrane to study the capacity of proteins/peptides to approach and penetrate the lipid membrane, an essential step in the action of bioactive peptides (Boisselier et al., 2017; Brockman, 1999; Fidelio et al., 1986; Maget-Dana, 1999). This model system allows close control of the biophysical properties of the lipid film such as surface pressure, phase state and surface topography, keeping a planar topology for any membrane composition (Wilke, 2014). It also allows direct visualization of heterogeneous membranes and their evolution with a change of surface molecular density and/or membrane composition (Fanani et al., 2010).

The incorporation of amphiphilic peptides induces lateral compression of the membrane components, increasing the surface molecular density and thus its surface pressure (Maget-Dana, 1999). The membrane phase state has also been observed to influence peptide/protein incorporation into lipid membranes, as well as the incorporation of smaller amphiphilic molecules (Zulueta Diaz et al., 2016; Zulueta Díaz and Fanani, 2017). However, a clear pattern cannot be pictured; *e.g., Retinitis pigmentosa 2* shows evidence of a stronger interaction with PC membranes in the liquid-condensed (LC) or solid state than with more fluid liquid-expanded (LE) membranes (Boisselier et al., 2012). On the other hand, several phospholipases (De Tullio et al., 2008; Gudmand et al., 2010), as well as the pore-forming toxin *Sticholysin I* (Pedrera et al., 2014) and several antimicrobial peptides (Dyck et al., 2006; Polozov et al., 1997), penetrate largely into LE membranes, and are sensitive to a diminishing of membrane fluidity.

Recently, we explored the interfacial properties of MP1 at air-water and air-saline solution interfaces by using Langmuir monolayers and their interaction with the zwitterionic phospholipid, dipalmitoylphosphatidylcholine (DPPC) (Alvares et al., 2016). A more favorable interaction was evidenced with the phospholipid membrane in the LE state than in the LC phase. Furthermore, the concomitant presence of acidic and basic residues in the MP1 sequence resulted in peptide–-peptide and peptide-lipid interactions finely tuned by aqueous ionic strength and pH.

The present work explores MP1 interaction with negatively charged PS monolayers in comparison to those formed by the zwitterionic lipid, phosphatidylcholine (PC). PC is the most abundant phospholipid in cell membranes. Within this lipid family, the PC that contains two saturated acyl chains of 14C (dimyristoylphosphatidylcholine, DMPC) is widely used for forming model lipid bilayers (liposomes) because it exhibits a liquid-disordered phase at 37 °C, the lipid phase that best represents average cell membrane behavior (Heimburg, 2007). DMPC is also able to form an LE phase in monolayers over the whole surface pressure range at room temperature (Vega Mercado et al., 2011). We studied the insertion of MP1 into DMPC monolayers to assess its interaction with a neutral LE lipid film, and comparatively, MP1 behavior against DPPC monolayers, which show LE-LC phase coexistence. The interaction of MP1 with negatively charged films was explored by using PS monolayers exhibiting different phase states: dioleoylphosphatidylserine (DOPS) exhibits only LE phase, dimyristoylphosphatidylserine (DMPS) shows LE-LC phase coexistence, whilst dipalmitoylphosphatidylserine (DPPS) shows only an LC-like phase.

MP1's capacity to penetrate lipid films correlated with changes in phase state and domain texture of the lipid monolayers as observed by Langmuir compression isotherms and Brewster angle microscopy (BAM). The electrostatic properties of the peptide-anionic lipid mixed films were explored, analyzing the effect of the ionic strength in all experiments. Our results showed a strong capacity of MP1 to regulate phospholipid phase transitions, which in turn influence its incorporation into the membrane.

2. Materials and method

2.1. Chemicals and reagents

The lipids, 1,2-dioleoyl-*sn*-glycero-3-phosphoserine (DOPS), 1,2 dimyristoyl-sn-3-glycerophosphoserine (DMPS), 1,2-dimyristoyl-sn-3-glycerophosphocoline (DMPC), 1,2-dipalmitoyl-sn-3-glycerophosphoserine (DPPS) and 1,2-dipalmitoyl-sn-3-glycerophosphocoline (DPPC), were purchased from Avanti Polar Lipids (Alabaster − AL, USA). The lipids were used without any further purification. The peptide, Polybia MP-1 (MP1), was from BioSynthesis (Lewisville- TX- USA) with RP-HPLC purity level > 98%. Chloroform and methanol, HPLC grade, were obtained from Merck (Darmstadt, Germany). Sodium chloride and sodium hydroxide were from Sigma-Aldrich. Ultrapure water used for the preparation of the subphases was previously deionized in ion exchange resin and then filtered in a Millipore Milli-Q system (Direct-Q UV, Merck Millipore, Darmstadt, Germany). The specific resistance was ~18 MΩ cm. All experiments were performed in ultrapure water or saline solution (150 mM NaCl, pH 7.4) at 20 °C.

2.2. Adsorption and insertion experiments

The adsorption of the peptide to the air-water interface, as well as its insertion into preformed lipid monolayers, were assessed in experiments at constant area using a home-made circular trough (surface area = 7 cm^2, volume = 4.5 ml). Adsorption experiments were performed by injecting increasing volumes of MP1 diluted in water (or saline solution) into the aqueous subphase under continuous stirring. The change in surface pressure (Δp) was registered as a function of time.

The surface activity curves (Δπ vs peptide concentration (c)) were fitted via non-linear least-squares regression analysis as described in the Supplementary material. The peptide adsorption curves allow the calculation of the peptides' surface excess concentration (Γ) by applying the Gibbs adsorption equation:

$$\Gamma = (1/RT)(\Delta\pi/\Delta Inc) \quad (1)$$

where R is the gas constant and T is the temperature. Using the peptide maximum surface excess concentration, the molecular area can be calculated as $A = 1/N\Gamma_{max}$, where N is Avogadro's constant.

Peptide insertion into phospholipid monolayers was determined by spreading the phospholipid from a solution in chloroform:methanol (2:1 v:v) onto the air-water (or air–150 mM NaCl) interface until reaching the desired initial surface pressure (π_i). Then, the peptide was injected into the subphase under continuous stirring at a final concentration of 1.25 μM. The insertion of the peptide into the monolayers was followed by the increase in surface pressure as a function of time. All experiments were performed at 20 °C.

2.3. Compression isotherms

Compression isotherms of lipids or lipid/peptide mixture were carried out in a Teflon trough (volume 180 ml, surface area 243 cm^2) containing water or saline solution (150 mM NaCl, pH 7.4). The surface pressure (π) was determined with a Pt plate by the Wilhelmy method, and the total film area was continuously registered using a KSV Minitrough apparatus (KSV, Helsinki, Finland) enclosed in an acrylic box. For lipid or lipid-peptide mixed monolayers, phospholipids were

dissolved in chloroform/methanol (2:1 v:v) to a final concentration of 2.5 mM and peptides were dissolved in methanol. Small drops of lipid or lipid-peptide premixed at a desired ratio were directly spread onto the aqueous surface. Monolayers were compressed at a velocity of 2.5 $Å^2$ $molecule^{-1}$ min^{-1}. The organic solvents were allowed to evaporate for 10 min before compression. All measurements were performed at 20 °C. The mean molecular areas determined were highly reproducible, with standard deviations lower than 3%, obtained from at least three compression isotherms for each condition.

2.4. Brewster angle microscopy (BAM)

To monitor the surface morphology of the monolayer, the Langmuir films were prepared as described above, in a trough previously mounted on the stage of a Nanofilm EP3 Imaging Ellipsometer (Accurion, Goettingen, Germany), working in the Brewster angle microscopy mode. Minimum reflection was set with a polarized laser (λ = 532 nm) incident on the bare aqueous surface at the experimentally calibrated Brewster angle (~53.1°). After monolayer formation and during compression, the reflected light was collected through a 20× objective. Further image analysis was performed using the NIH free software Image J. For better visualization of the images, the gray level range was reduced from an original range of 0–255 to 0–80. The reflectivity (R) is the ratio of the reflected intensity (I_R) after interacting with the surface, over the incident (I_o) ($R = I_R/I_o$), and the R of each phase of the film was calculated from the gray level average values of each phase of the BAM images by the following relation:

$$R = (\text{graylevel} - 13.6)\cdot f_c \quad (2)$$

where f_c, the calibration factor ($\sim 10^{-7}$), is the slope of the plot that relates the reflectivity with the average gray level of the images captured after a laser beam (p-polarized) is reflected by a bare air/water (or saline subphase) interface, which was checked for each experiment, and 13.6 is the average dark signal (background gray level in the absence of the monolayer). The reflectivity at the Brewster angle increases with the film thickness (l) and the refraction index of the film (n_f) and the subphase (n_s). The values of R, n_f and n_s enabled the film thickness of each phase and the film of pure peptide to be estimated. Since it is not trivial to determine n, we chose 1.45 for the peptide, as was used in other studies for the Annexin A5 peptide (Fezoua-Boubegtiten et al., 2010), whilst 1.45 was used for DMPC, DOPS and DMPS and 1.48 for DPPS films (Fezoua-Boubegtiten et al., 2010; Kienle et al., 2014). R is related to the square of l as reported in Pusterla et al. (2017).

2.5. Atomic force microscopy (AFM)

The transferred monolayers were prepared as detailed in Mangiarotti et al. (Mangiarotti et al., 2014). Briefly, the hydrophilic substrates (glass coverslips) were treated with piranha solution (H_2SO_4:H_2O_2 3:1 v/v) at 90 °C for 60 min and rinsed with Milli-Q water. Then, a solution of lipid and MP1 (7.2 mol% of MP1) was spread onto the water surface and compressed up to 15 mN/m. The monolayer was allowed to stabilize (~100 s), and was then transferred by the Langmuir–Blodgett (LB) technique to the previously submerged substrate (oriented perpendicular to the trough) at a rate of 5 mm/min, while maintaining the surface pressure constant. The supported monolayers remained exposed to air during the experiments. A transfer ratio in the range of 1.1 (± 0.1) was obtained. An AFM Innova atomic force microscope (Bruker, Billerica, Massachusetts) was used to obtain AFM images in the tapping mode, using a silicon probe with a nominal spring constant of 40 N/m and a resonance frequency of 300 kHz at room temperature (~20 °C).

2.6. Ionization state of DMPS and DPPS at different ionic strengths

Anionic lipid monolayers induce the formation of an ionic double layer, thus attracting protons to the surface, and inducing a decrease in the surface pH (pH_{sf}). Therefore, the surface pH differs from the bulk pH (pH_{sb}) by

$$pH_{sf} = pH_{sb} + F\psi_0/(2.3RT) \quad (3)$$

where F is the Faraday constant, ψ_0 is the double layer potential at the surface and RT is the thermal energy (Gaines, 1966). The double layer potential depends on the ionic strength of the subphase and on the degree of ionization (α) of the lipid molecules, and therefore the surface charge density (σ) is related to ψ_0, with a mutual regulation being established (Wilke, 2014). Since there is no analytical solution, a numerical approach was used as described by Vega Mercado (Vega Mercado et al., 2011) to obtain the pH_{sf} and α for water or saline subphase.

3. Results

3.1. Surface activity of MP1 and its insertion into phospholipid monolayers

The surface activity of MP1 was examined at the air-water and air-NaCl solution interfaces, monitoring the increase in surface pressure as a function of time (Fig. 1A and B, respectively). The adsorption kinetics of the peptide onto a clean interface show that MP1 adsorbed in a very short time onto the air-NaCl solution interface (< 50s). However, MP1 took more than 500 s after its injection into pure water to induce a significant change in the surface pressure, a phenomenon previously reported for *Retinitis pigmentosa 2* or RP2 (Boisselier et al., 2012). MP1 has two aspartic acids concomitantly with three lysines and the amidated C-terminus, conferring a positive net charge (+2e) at physiological pH values. Thus, an enhanced electrostatic repulsion occurring in pure water between the newly-formed charged film and the soluble peptides near the surface may be responsible for a hindered penetration kinetic in such conditions. Interestingly, in saline solution, the surface

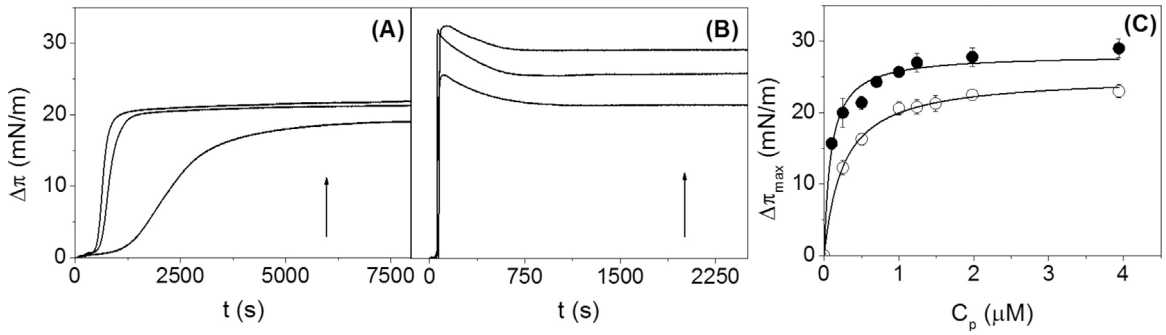

Fig. 1. (A and B) Adsorption kinetics of peptide (in different concentrations ↑ from bottom to top 0.5, 1.0 and 1.25 μM) into air-water and air-NaCl solution interfaces, respectively. (C) The maximum change of surface pressure as a function of peptide concentration injected on pure water (open symbols) and ionic solution (closed symbols). The data represent the average ± the standard error of at least three independent measurements. The continuous lines represent the non-linear least-squares regression analysis.

Table 1
Physicochemical properties of MP1 films.

Subphase	π_{col} [a]	π_{max} [b]	Γ_{max} [c]	A [d]	A [e]
	(mN/m)	(mN/m)	($\times 10^{-6}$ mol/m^2)	(nm^2/molecule)	(nm^2/molecule)
Pure water	17 ± 1	25.1 ± 0.4	0.85 ± 0.08	2.0 ± 0.2	1.6 ± 0.2
150 mM NaCl	19 ± 1	28.1 ± 0.8	0.96 ± 0.06	1.7 ± 0.2	2.2 ± 0.2

[a] Collapse pressure of MP1 films obtained from compression isotherm. Extracted from Alvares et al. (2016).
[b] Maximum surface pressure obtained via non-linear least-squares regression analysis of curve approaching a rectangular hyperbola (Fig. 1C).
[c] The peptide surface excess concentration calculated by applying Eq. (1).
[d] Molecular area at maximum adsorption, calculated using the peptide maximum surface excess concentration.
[e] Molecular area obtained from the compression isotherms, extracted from Alvares et al. (2016) at maximal compaction in each case (17 and 19 mN/m, without and with NaCl respectively).

pressure showed a maximum value, after which it decreased and remained constant. This behavior has been related with film rearrangements as the amphiphile forms a Gibbs monolayer (Maget-Dana, 1999; Vollhardt and Fainerman, 2010). The rearrangements may be due to surface electrostatic changes caused by the peptide adsorption, as previously reported for other ionizable amphiphiles (Mottola et al., 2013). However, this rearrangement occurs only in the presence of salt, where electrostatic interactions are screened. In this condition, the amount of peptide at the interface is higher, probably reaching the conditions for the suggested rearrangement.

Fig. 1C shows the maximum change of surface pressure as a function of peptide concentration injected into pure water and ionic solution. It can be seen that the maximal surface pressure increased with the increase of peptide concentration and the maximum value was reached at 1.5–2.0 μM MP1 in both subphases. The values of $\Delta\pi_{max}$ and Γ_{max}, shown in Table 1, were calculated applying Eqs. S1 and 1, respectively. From the values of Γ_{max}, we calculated the mean area per adsorbed molecule, a parameter that is compared (in the Discussion section) with the molecular area measured from Langmuir film compression experiments (π_{col}) (see Table 1).

We further explored the interaction of MP1 with phospholipid monolayers by monitoring the time course for equilibration of MP1 injected into the subphase of a pre-formed lipid film (see Fig. S1 in Supplementary material). The affinity of MP1 to lipid monolayers was investigated, measuring its ability to insert into a lipid film differing in the acyl chain length and unsaturation, and as a consequence, the film phase state and density. Fig. 2 shows the maximum change of surface pressure ($\Delta\pi_{max}$) induced by MP1 as a function of the initial surface pressure (π_i) of the anionic DOPS, DMPS, and DPPS or neutral DMPC and DPPC monolayers formed onto pure water or 150 mM NaCl, pH 7.4. For these experiments, we used the peptide bulk concentration in which ~90% of saturation was reached and the peptide acquired a significant surface activity (1.25 μM, see Fig. 1C).

As can be observed in Fig. 2 for MP1, and as is general behavior for amphiphile insertion into lipid films (Boisselier et al., 2017; Brockman, 1999; Maget-Dana and Ptak, 1995), the surface pressure increases due to peptide insertion and decreases with an increment of the initial surface pressure of the lipid film. This results in linear $\Delta\pi_{max}$ vs. π_i plots with negative slopes. By extrapolating the linear regression to $\Delta\pi_{max}$ = 0 mN/m, the exclusion pressures, π_e (Bougis et al., 1981; Maget-Dana and Ptak, 1995), were determined for the experiments shown in Fig. 2 (Table 2). The value of π_e indicates the pressure above which no more peptide molecules penetrate the lipid monolayer. Since it has been proposed that bilayers and monolayers are comparable for lateral pressure values in the range of 30–35 mN/m (Marsh, 1996), π_e can be used to estimate the capacity of bioactive peptides to penetrate target cell membranes (Brockman, 1999).

Our results indicated that π_e varies in the range of 35–42 mN/m for DOPS and DMPS on both water and saline solutions, values that exceed the surface pressures comparable to lipid bilayers. MP1 can be incorporated into DPPS, DMPC, and DPPC up to lower surface pressures. For DPPS and DMPS films, the high ionic strength hinders the electrostatic attraction between the cationic peptide and the anionic lipid monolayer, since the addition of NaCl decreases π_e. On the other hand, NaCl had a similar effect on MP1 penetration into the neutral PC monolayers as on its adsorption into a bare surface: a decrease of electrostatic repulsion due to high ionic strength reduces the interaction between the cationic peptide and the membrane, which becomes enriched in the adsorbed peptide, conferring a progressively higher cationic character along the adsorption time curve. In summary, the presence of salt subtly regulates the peptide penetration around the surface pressures of physiological relevance, inducing opposite effects in the anionic DPPS and DMPS compared to the neutral DMPC and DPPC.

3.2. Impact of MP1 on PS and PC monolayers in liquid-expanded phase

The penetration process of amphiphiles into the membrane involves the increasing enrichment of the lipid film with these until reaching thermodynamic equilibrium. In the present work, we were not able to measure the final amount of MP1 inserted into the lipid films. However, to investigate the properties of such binary systems, we studied mixed lipid/MP1 Langmuir films at different molar ratios. These are metastable two-dimensional films, which are not in equilibrium with the subphase but behave as stable systems during the experimental time (Gaines, 1966).

The compression isotherms of both pure DMPC and pure DOPS reveal a fluid-like state in water and in 150 mM NaCl (Fig. 3). The presence of 7.2 mol% of MP1 at the interface induced an increase in the area corresponding to the isotherm lift-off for all cases (note that the x-axis values correspond to the area per lipid molecule, without considering the number of peptide molecules). The presence of the peptide induced an area expansion of ~14% for DMPC in both subphases at 15 mN/m, and for DOPS, of 16% in water and of 23% in the saline subphase at the same surface pressure. Assuming ideal mixing behavior, MP1 is expected to occupy 12–15% of the lipid monolayer area at 15 mN/m (see Alvares et al., 2016), and accordingly a moderate expansion of the film was found for DOPS/MP1 mixtures in saline solution.

For films containing DMPC, a plateau is present in the 22–30 mN/m pressure range. Above this pressure, the isotherm becomes similar to that of the pure lipid, strongly suggesting the exclusion of peptide molecules from the interface (Alvares et al., 2016; Birdi, 2006; Maget-Dana, 1999). This phenomenon occurs at a surface pressure 5 mN/m lower in water than in NaCl solution (Table 2), indicating that an in-plane electrostatic repulsion between the cationic peptides is one of the factors that promote its desorption from the interface. Notably, for DOPS films a plateau that would evidence expulsion of the peptide was not observed, indicating that the favorable PS–MP1 interaction (probably of electrostatic nature) may be responsible for their being able to withstand the lateral pressure and reach the collapse process of the film as a binary mixture (Fig. 3). It should be noted that this collapse

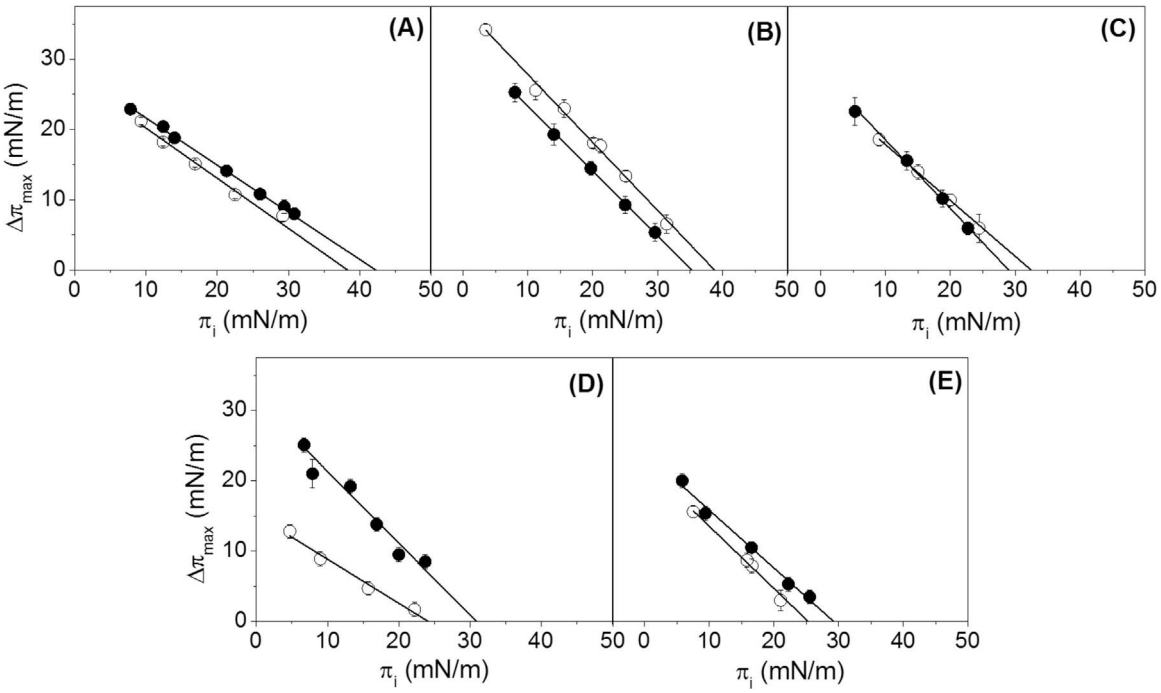

Fig. 2. Peptide insertion into lipid monolayers: the maximum change of surface pressure ($\Delta\pi_{max}$) after injection in the subphase of peptide (1.25 μM) measured as a function of initial pressure (π_i) of DOPS (A), DMPS (B), DPPS (C), DMPC (D) and DPPC (E). The subphase was pure water (open symbols) or 150 mM NaCl (closed symbols). The data represent the average ± the standard error of at least three independent measurements. The continuous lines represent the linear regressions.

occurred at a surface pressure ~26 mN/m higher than that for the pure peptide film (Table 1), suggesting a strong molecular interaction between the peptide and the anionic lipid in the LE phase state.

3.3. Impact of MP1 on PS monolayer with LE-LC coexistence phase

Fig. 4A shows that the compression isotherm for DMPS films at the air-water interface depicted a characteristic plateau, at ~1.4 mN/m indicating the coexistence of LE and LC phases at 20 °C, in good agreement with the results obtained by Dyck and Losche (Dyck et al., 2006).

For mixtures containing peptide, the area per lipid molecule at surface pressures below ~30 mN/m was displaced to larger values. For 2.4 mol% of MP1, this represents ~ 11% of area increase at 15 mN/m, which is expected to occupy only 8.2% of the monolayer area assuming ideal mixing behavior. The positive deviation was observed in all lipid/peptide ratios, indicating a non-ideal mixing behavior, also evidenced by an increase in the LE-LC transition surface pressure (from 1.4 to 3.0 mN/m) induced by MP1. The collapse of the peptide-enriched phase occurred at ~15 mN/m higher than the collapse of the pure peptide film. Surprisingly, above 7.2 mol% of peptide, the area per lipid molecule at surface pressures above 35 mN/m shifted to values lower than those observed for the pure lipid, suggesting that part of the film (lipid and peptide) was lost from the interface. This may be a consequence of a very strong DMPS-peptide attractive interaction.

Compression-expansion cycles of DMPS/MP1 monolayers were performed to explore the reversibility of the transitions observed (see Fig. S2 in Supplementary material). Lipid films containing 6 mol% of peptides were compressed up to 15 mN/m, expanded and re-compressed. The area per lipid molecule remained unchanged after this treatment, evidencing a negligible loss of material from the interface. However, when the monolayer was compressed up to a surface pressure above the second plateau (60 mN/m), the film showed a partially reversible behavior, evidencing a relatively larger loss of material from the interface at low, but not at high, surface pressures. This effect was more evident for isotherms with 7.2 mol% of MP1 (compare Fig. S2A

Table 2
Comparison of the exclusion pressure and the collapse pressure for MP1 in PS and PC monolayers.

Subphase	Composition	Lipid film phase state [a]	Lipid/MP1 film phase state [a,b]	$\pi_{col}{}^{i}$ (mN/m)	$\pi_{col}{}^{f}$ (mN/m)	$\pi_{e}{}^{c}$ (mN/m)
Pure water	DOPS/MP1	LE	LE	43 ± 2	–	38 ± 1
	DMPS/MP1	LE-LC (2–12)	LE-LC (5–36)	32 ± 1	37 ± 1	39 ± 1
	DPPS/MP1	Gas − LC (< 3)	LE-LC (< 23)	23 ± 1	32 ± 2	32 ± 2
	DMPC/MP1	LE	LE	17	23	24 ± 2
	DPPC/MP1 [d]	LE-LC (4–15)	LE-LC (6)	18 ± 1	23 ± 2	26 ± 2
150 mM NaCl	DOPS/MP1	LE	LE	41 ± 2	–	42 ± 1
	DMPS/MP1	LE-LC (16–33)	LE-LC (19–39)	27 ± 2	41 ± 2	35 ± 1
	DPPS/MP1	Gas − LC (< 6)	LE-LC (< 29)	21 ± 1	29 ± 1	28 ± 1
	DMPC/MP1	LE	LE	25	30	31 ± 2
	DPPC/MP1 [d]	LE-LC (4–11)	LE-LC (4–24)	21 ± 2	29 ± 2	29 ± 2

[i] initial and [f] final surface pressure for the collapse of the MP1-enriched phase process, obtained from compression isotherm shown in Figs. 4–7.
[a] The phase coexistence surface pressure range is indicated between brackets, expressed as average ± 1 mN/m, obtained from BAM images.
[b] The data corresponds to an MP1 content of 7.2 mol%.
[c] The exclusion pressure was obtained from insertion experiments (Fig. 2).
[d] Extracted from (Alvares et al., 2016).

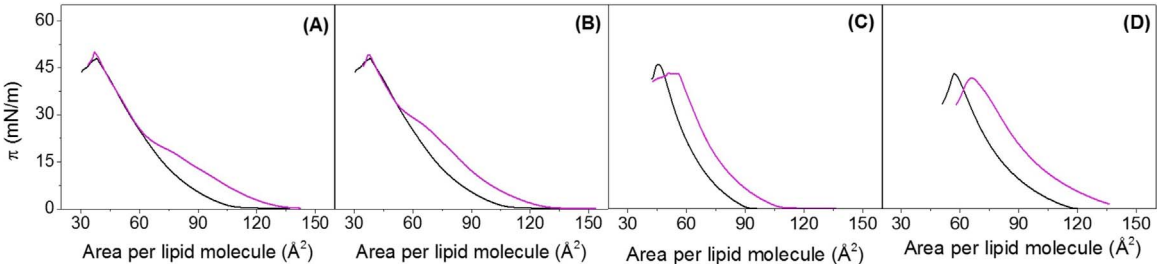

Fig. 3. Surface interaction of MP1/DMPC and MP1/DOPS monolayers in the LE phase state. (A–B) Surface pressure-area compression isotherms for pure DMPC (black lines) or co-spread with MP1 7.2 mol% (colored line). (C–D) Surface pressure-area compression isotherms for pure DOPS (black lines) or co-spread with MP1 7.2 mol% (colored line). The subphases used were water (A–C) or NaCl 150 mM, pH 7.4 (B–D) surface. The monolayers were compressed at 5 cm2/min, T = 20 °C. The curves are representative experiments, varying less than 2 mN/m from their corresponding replicates.

and B). This result indicates that the process involved in the second plateau correlates with a partially reversible collapse at the compression rates employed.

Brewster angle microscopy enabled the formation and growth of lipid domains and the changes of the optical properties of the interface, such as refractive index and film thickness (Pusterla et al., 2017) to be investigated in the presence of the peptide. Thus, films in the LE phase state are usually thin because the lipid chains are partially stretched laterally, occupying a large area and have a low refractive index, appearing as dark gray regions. On the other hand, films in the LC phase state are thicker, due to the upright position of the acyl chain and a more compact lipid configuration, resulting in a higher refractive index and are observed as brighter gray areas (Daear et al., 2017). Representative BAM micrographs of the pure DMPS films at the air-water interface are shown in Fig. 4B. The images show the presence of large LC domains with dendritic-shapes. Domains appear at 1.5 mN/m, matching the starting point of the plateau corresponding to the phase transition in Fig. 4A. The LC domains grew upon further compression so that, at 15 mN/m, all the regions corresponding to the LE phase almost completely disappeared (less than 1% of LE phase remained).

4.8 mol% of MP1 (co-spread with DMPS) (Fig. 4C) induced a slight increase in the LE-LC transition surface pressure (~2 mN/m) compared to pure lipid films, strongly suggesting a more favorable DMPS/MP1 surface mixing in the LE phase state. In the presence of MP1, the domains appeared smaller and in larger numbers, and the LE phase coexisted with the LC phase up to surface pressures of ~37 mN/m. Furthermore, at 15 mN/m, the percentage of area occupied by the LE phase reached 41 ± 2%, much larger than the ~16% expected to be occupied by the peptide alone. This, together with the fact that the LE-LC coexistence region shifted to higher surface pressure, suggests that MP1 was preferentially located in the LE phase, which was probably composed of peptides and lipids molecules. White dots can be observed in BAM images (Fig. 4 and 5), which correspond to out-of-plane (three-dimensional) lipid or lipid/peptide structures that protrude from the film to an extent exceeding the resolution of the technique (> 10 nm). The presence of such white dots may reflect a tendency of the membrane to form highly curved structures.

Further addition of MP1 to the DMPS films (7.2 mol%, Fig. 2D) induced even smaller condensed domains, suggesting that the presence of the peptide favors the nucleation process against domain growth, acting as seeds, lowering the line tension and/or decreasing the diffusion of the molecules to the growing domain (Rosetti et al., 2017). The image inserted in Fig. 4D shows an AFM image of this film transferred onto glass at 15 mN/m, where the domains can be observed at a better

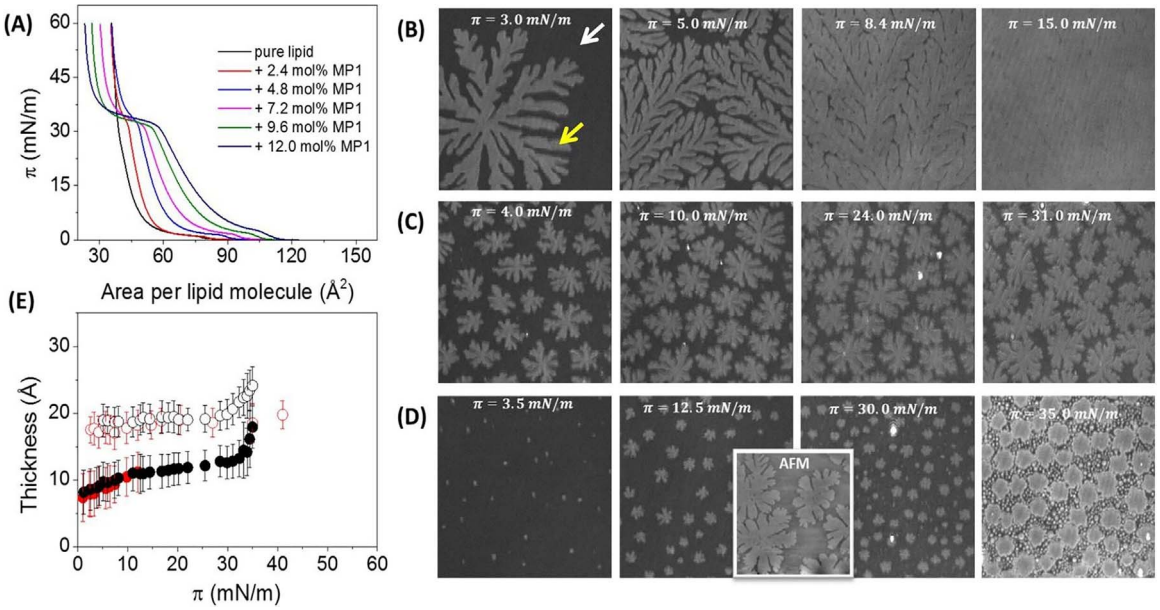

Fig. 4. DMPS/MP1 surface interaction (pure water): (A) surface pressure-area compression isotherms for DMPS co-spread with increasing amounts of MP1 onto the water surface. The monolayers were compressed at 5 cm^2/min, T = 20 °C. (B–D) Representative BAM images for monolayers of pure lipid (B), and for mixtures of DMPS and 4.8 and 7.2 mol% of MP1, (C-D) respectively, spread onto pure water and registered during compression at the indicated surface pressures. The arrows indicate the area occupied by LE (white) or LC (yellow) phases. Image size: 200 × 200 μm^2. The inset image represents the AFM image with image size 100 × 100 μm^2. (E) Monolayer thickness of dark region (close symbols) and light region (open symbols) calculated from BAM images of pure lipid (red) and lipid/peptide for 7.2 mol% of MP1 (black) films. (For interpretation of the references to colour in this figure legend, the reader is referred to the web version of this article.)

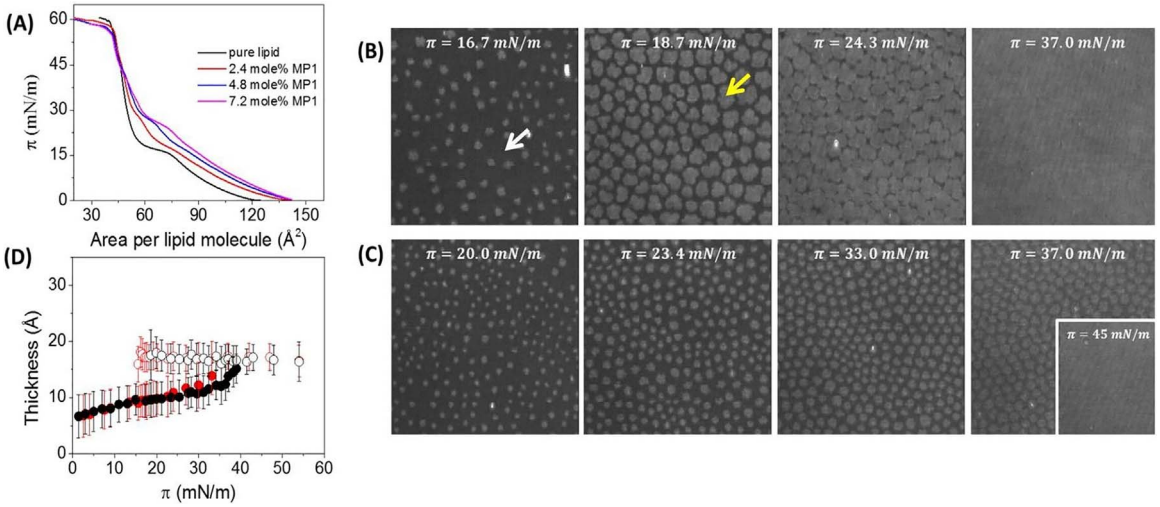

Fig. 5. DMPS/MP1 surface interaction (NaCl): (A) surface pressure-area compression isotherms for DMPS co-spread with increasing amounts of MP1 onto the saline solution. The monolayers were compressed at 5 cm^2/min, T = 20 °C. (B and C) Representative BAM images for monolayers of pure lipid (B) and a mixture of DMPS and 7.2 mol% of MP1 (C) spread on the saline solution and registered during compression and at the indicated surface pressures. The arrows indicate the area occupied by LE (white) or LC (yellow) phases. Image size: 200 × 200 μm^2. (D) Monolayer thickness of dark region (close symbols) and light region (open symbols) calculated from BAM images of pure lipid (red) and lipid/peptide for 7.2 mol% of MP1 (black) films. (For interpretation of the references to colour in this figure legend, the reader is referred to the web version of this article.)

resolution.

A further increase of the surface pressure led to a second nucleation of domains (see Fig. 4D at 30 mN/m) and at higher surface pressure, the borders of the condensed domains became brighter. This increased its reflectivity compared with pure lipid films, indicating an increase in the thickness of the films (Fig. 4E), surpassing that of a single monolayer. This effect may correspond to 3D structures formed by lipids and peptides reversibly associated with the interface (as suggested by the compression/decompression experiments shown in Fig. S1), which would explain the decrease in the mean molecular area at high pressures depicted in the compression isotherms (Fig. 4A).

To check whether this lipid-peptide 3D aggregation was promoted by electrostatic lipid-peptide interactions, similar experiments were performed on saline solutions. On a subphase containing 150 mM NaCl, the compression isotherm of the pure lipid was displaced to higher molecular areas and the coexistence phase plateau appeared at surface pressure ~16 mN/m (Fig. 5A), at which the formation of smaller and rounder LC domains occurred (Fig. 5B). PS has an ionizable headgroup with a pKa of 3.6 (Tsui et al., 1986). When the molecules self-organize in an ionized monolayer, a charged plane is generated with the corresponding formation of an ionic double layer. As previously described, this leads to a decrease in the surface pH, to an extent that depends on the ionic strength of the solution (Gaines, 1966). Thus, the higher the ionic strength, the lower is the change in surface pH, compared with that in bulk (Wilke, 2014). Therefore, in the presence of salt, the surface pH of pure DMPS monolayers is expected to be close to that in the solution (i.e. 7.4), whilst in the absence of salt, it is expected to be lower.

The values of the surface pH were estimated for DMPS monolayers at high film compaction, as described in Vega Mercado et al. (Vega Mercado et al., 2011), using the Gouy-Chapman model for a bulk pH of 7.4 and assuming a pKa value of 3.6 (Tsui et al., 1986). We found a surface pH of ~2 on water and ~5.5 on 150 mM NaCl, which corresponds to dissociation degrees of 2% and 99% of the headgroups, respectively; i.e. on water the PS moieties were mostly neutral and on NaCl, mostly charged. This promoted a higher intermolecular repulsion in the presence of salt. It is known that changes in the ionization state of lipid molecules lead to changes in lipid packing (Tocanne and Teissie, 1990), and therefore, the change in the isotherms of the pure lipids induced by NaCl may be a consequence of the change in the ionization state of the film.

In the mixed films, the presence of the peptide decreased the charge density of the monolayer, and thus the decrease in the surface pH would not be so marked. The approach employed here for the calculation of the surface pH assumes a homogeneous distribution of charges at the surface, and thus it may be valid for the PS moieties located far away from the peptide, but not for PS in the peptide proximity. Therefore, a similar reasoning is not valid for PS molecules interacting with the peptides, and we expect that the degree of ionized PS surrounding the MP1 molecules was close to 100% in both water and NaCl solutions.

When the peptide was co-spread with the lipid, the LE-LC phase transition was shifted to 19 mN/m and the plateau corresponding to the peptide collapse took place at ~ 41 mN/m (Table 2), reflecting a favorable peptide-anionic membrane interaction. Superposition of the isotherms was observed at surface pressures > 41 mN/m, indicating that, after this plateau, almost all the peptide molecules were squeezed out to the subphase.

On ionic solution, the peptide also preferred the LE phase, thereby increasing the area extent of this phase (from 9 ± 1 to 83 ± 4% at 23 mN/m, compare Fig. 5B and C). The average size of the domains was smaller than those for the pure lipid monolayer, whilst the thickness of the film remained similar (Fig. 5D). This observation, together with the behavior of the mixed isotherms, indicates the absence of lipid/peptide 3D aggregation. Therefore, we conclude that the interaction between PS lipids and the peptide has an electrostatic component, which loses importance in the presence of salt. To check whether the hydrocarbon chain and lipid film thickness is also a modulator of the lipid-peptide interaction, mixed monolayers of DPPS and the peptide were prepared and studied.

3.4. Impact of MP1 on liquid-condensed PS films

In the compression isotherms of pure DPPS, only gas–LC phases were evidenced at very low surface pressures, lacking the LE-LC phase coexistence region in water and in 150 mN NaCl solution (Bouffioux et al., 2007; Chen et al., 2010) (see Figs. 6A and 7A , respectively). On water, the presence of MP1 induced similar changes to those observed with the DMPS/MP1 mixture. But the near-superposition of isotherms at surface pressure > 28 mN/m (~9 mN/m lower than that observed in DMPS/MP1 films) indicated that the peptide molecules were squeezed out to the subphase, dragging fewer lipid molecules, compared with DMPS/MP1 films (compare Figs. 6A and 4A). However, it must be

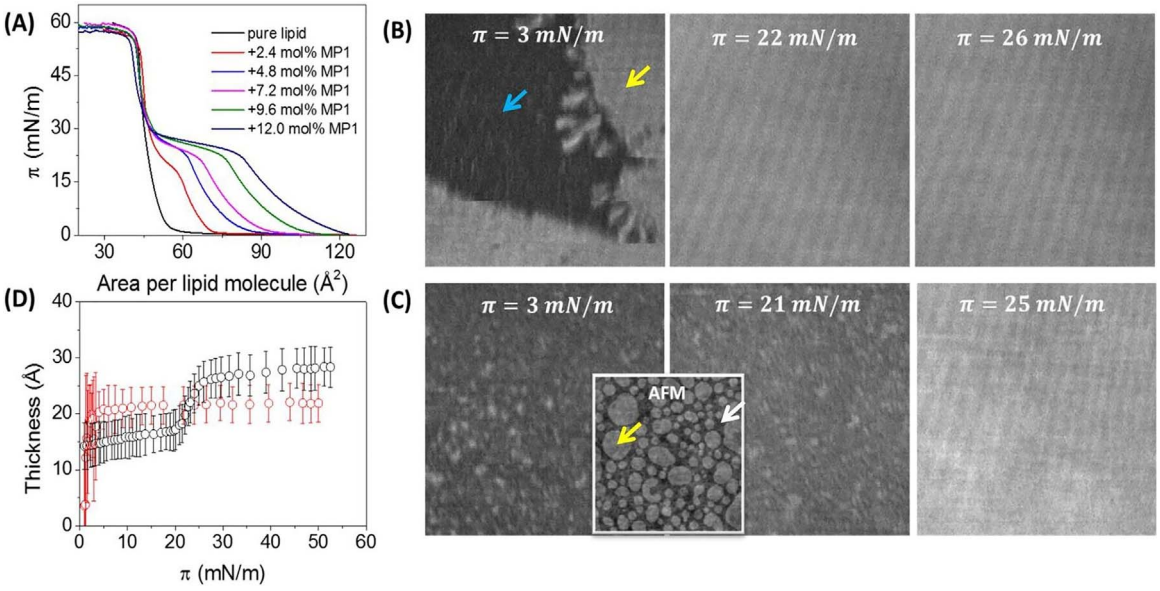

Fig. 6. DPPS/MP1 surface interaction (pure water): (A) surface pressure-area compression isotherms for DPPS co-spread with increasing amounts of MP1 onto the water surface. The monolayers were compressed at 5 cm^2/min, T = 20 °C. (B and C) Representative BAM images for monolayers of pure lipid (B) and a mixture of DPPS and 7.2 mol% of MP1 (C), spread on pure water and registered during compression and at the indicated surface pressures. The arrows indicate the area occupied by the gas (light blue), LE (white) or LC (yellow) phases. Image size: 200 × 200 μm^2. The inset image represents the AFM image with image size 10 × 10 μm^2. (D) Average monolayer thickness calculated from BAM images of pure lipid (red symbols) and lipid/peptide for 7.2 mol% of MP1 (black symbols) films. (For interpretation of the references to colour in this figure legend, the reader is referred to the web version of this article.)

noted that the in-plane interaction between the lipid molecules in the DMPS films is less strong than in DPPS films, and it is thus easier for the DMPS molecules to escape from the monolayer. This accounts for the easier squeezing out of lipids in DMPS than in DPPS monolayers.

The BAM images reported in Fig. 6B show that, under our experimental conditions, gas-LC coexistence was observed at very low surface pressure, which became a uniform LC phase at a surface pressure > 3 mN/m. In mixed films of DPPS with 7.2 mol% of MP1, BAM images showed phase coexistence with small, blurred LC domains that were visible at surface pressures below the peptide expulsion pressure, surrounded by a dark gray area that corresponded to an LE phase (Fig. 6C). The latter remains present until reaching ~ 23 mN/m. The higher resolution of AFM enabled condensed domains to be seen, shown as an insert in Fig. 6C.

Fig. 6D shows that, in the presence of MP1, the film thickness at pressures below 20 mN/m was lower than for pure lipid films, whilst above 25 mN/m it was higher, reflecting a thicker film. This suggests that, at low surface pressures, where MP1 was incorporated into the monolayer, the films were on average thinner than pure DPPS, with the peptide molecules probably occupying the darkest gray (LE) regions in Fig. 6C. A closer analysis of the isotherms shown in Fig. 6A indicates that the area per lipid molecule increased by ~48% at 15 mN/m when

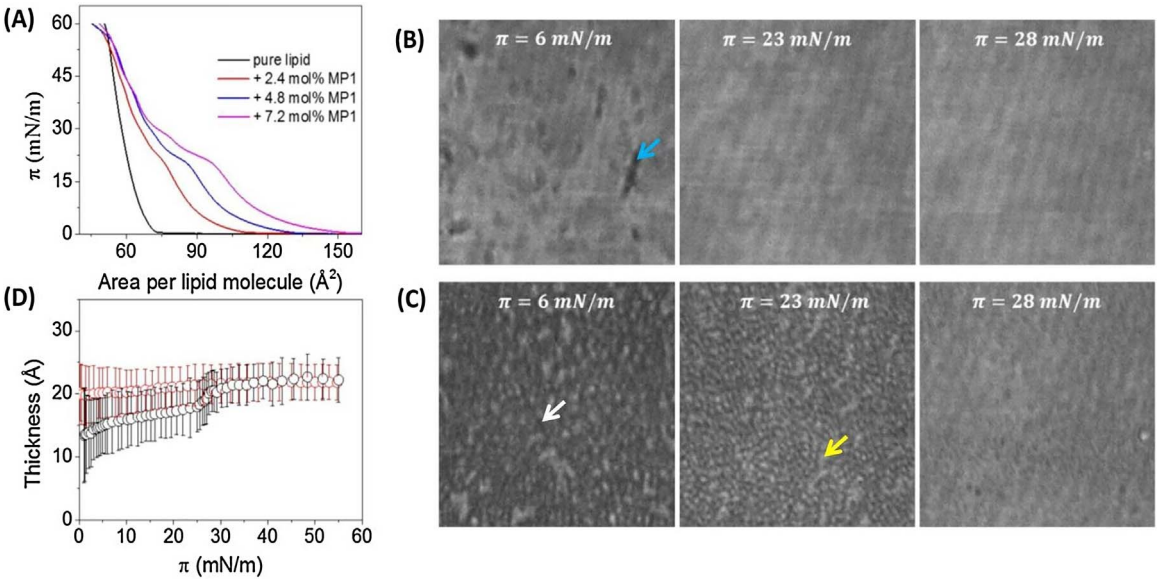

Fig. 7. DPPS/MP1 surface interaction (NaCl): (A) surface pressure-area compression isotherms for DPPS co-spread with increasing amounts of MP1 onto the saline solution. The monolayers were compressed at 5 cm^2/min, T = 20 °C. (B and C) Representative BAM images for monolayers of pure lipid (B) and a mixture of DPPS and 7.2 mol% of MP1 (C) spread on the saline solution and registered during compression and at the indicated surface pressures. The arrows indicate the area occupied by the gas (light blue), LE (white) or LC (yellow) phases. Image size: 200 × 200 μm^2. (D) Average monolayer thickness calculated from BAM images of pure lipid (red) and lipid/peptide for 7.2 mol% of MP1 (black) films. (For interpretation of the references to colour in this figure legend, the reader is referred to the web version of this article.)

7.2 mol% of the peptide was present, whilst the peptide alone is expected to occupy only 21% (assuming ideal mixing behavior and a transmembrane conformation). The area expansion observed may be explained by the peptide adopting a conformation parallel to the interfacial plane or inducing a proportion of lipids to transition to the LE phase (Fig. 6A and C), thus occupying a larger area. At high surface pressures, once the peptides are expelled from the monolayer, they remained associated to the lipid headgroups, forming a thicker interface (Fig. 6D).

Next, we studied the effect of salt on the DPPS/MP1 system (Fig. 7). On saline solution, the compression isotherms of mixed films showed two plateaus, one at 21 mN/m that correlated to the collapse pressure of pure peptide films and another at ~29 mN/m (Fig. 7A). Interestingly, at this condition, the superposition of the isotherms at high surface pressures was not observed, indicating that some peptide molecules remained in the monolayer up to the collapse pressure of the mixed film.

The BAM images obtained for pure DPPS (Fig. 7B) show that the brighter phase (LC) is anisotropic in the monolayer plane, as is evidenced by subtle differences in its gray level. This behavior has been associated with a crystalline-like inner structure of the lipid molecules when the axis of the molecules is tilted to the membrane normal (Mottola et al., 2015). For DPPS with 7.2 mol% of MP1, the images were analogous to those on pure water (compare Figs. 6C and 7C). However, above 30 mN/m, the reflectivity of the DPPS/MP1 films have the same value of pure lipid monolayers (Fig. 7D), not showing a significant thickening of the film. At low pressures, MP1 induced the occurrence of thinner monolayers than DPPS in the LC state, while upon compression some peptide molecules were expelled to the subphase, and the remaining (mixed) monolayer behaved like pure DPPS films in the LC phase.

4. Discussion

In this work, we explored MP1-membrane interaction using lipid monolayers as a model system. This well-controlled system provided information about the first steps for the incorporation of this antimicrobial peptide into the membrane, i.e. approach to the surface, adsorption at the interface and finally integration into the membrane. MP1 displayed higher surface activity at the air-NaCl interface than in pure water. For the latter case, considering the ionizable nature of the peptides, after the adsorption of a few molecules, a charged film will be established inducing electrostatic repulsion, which may disfavor a highly dense peptide film. Again, these results match what was found for other cationic peptides (Boisselier et al., 2017; Nobre et al., 2015). Notably, the maximal adsorption pressure occurred at 8 mN/m (water subphase) or 9 mN/m (NaCl subphase) above the collapse pressure of pure peptide Langmuir films (Table 1). This may be explained by the different nature of both systems. For Langmuir films, the peptide was absent from the subphase, and thus collapse occurred with a destabilization of the monolayer structure and a loss of molecules to the subphase. For adsorption experiments, the subphase was a source of peptides, thus allowing equilibration between the films and the monomer in the subphase. Molecular adsorption here is always counteracting peptide desorption and equilibrium is reached, while the collapse in Langmuir monolayers corresponds to an out-of-equilibrium process.

Different values of mean molecular area were found from the isotherms compared to the adsorption curves at the same subphase, but always in the range of 1.6–2.2 nm^2/molecule. This can be explained considering that the area calculation in both approaches assumes that the peptides form a monolayer at the interface. While this is likely to be the case in the compression experiments for surface pressures lower than the collapse, this may not be the case in the adsorption experiments, where the peptides may adsorb in a different manner when the interface is free of amphiphiles than when the surface is already populated by other peptide molecules and can also form multilayers. In addition, it should be recalled that the areas obtained from the Gibbs isotherm correspond to higher surface pressure than those from the compression isotherms.

A negative charge and the overall surface electrostatic condition is not the only factor that affects MP1 insertion into lipid monolayers, particularly at the physiologically relevant ionic strength tested (NaCl 150 mM) (see Table 2). The π_e value was higher when the monolayer was in the LE fluid phase and decreased with the increase of lipid chain length and saturation, which favors the formation of LC phases. For the insertion of the first peptide molecules, what matters is the phase state and fluidity of the pure lipid monolayer. However, as the peptide molecules insert into the monolayer, they may affect the film properties, generating a lipid-peptide interface with different properties that further modulate the peptide insertion.

Even though insertion experiments and Langmuir lipid/peptide mixed films are physically different, it has been shown for several cases that the films formed by both methods are closely comparable (Mottola et al., 2015; Vollhardt and Fainerman, 2010). Table 2 shows that the exclusion pressure for insertion experiments (π_e) roughly correlates with the collapse of the peptide-enriched phase (π_{col}) for MP1/lipid mixed films. Furthermore, the higher π_e and π_{col} values (the higher peptide capacity of incorporating into membranes) occurred with the combined presence of an anionic film in the LE phase, evidencing a hindered insertion of films in an LC phase.

MP1 mixed preferentially with the lipids in the LE fluid phase in Langmuir films for all the studied systems. The physico-chemical bases of this behavior must be found in the concepts related to (three-dimensional) solutions. A solvent (in our case the lipids) allows the incorporation of a solute (peptide) with the thermodynamic benefit of increasing the solution entropy. However, when the solvent–solvent interaction is much stronger than the solvent-solute interaction, the solution becomes thermodynamically unfavorable. Then, lipid–lipid interaction becomes an important regulation point for peptide incorporation. This interaction is stronger in the LC phase (due mainly to a closer packing of the lipids and an enhanced van der Walls attraction) than in the LE phase, when the lipid molecules are further apart, occupying a larger area and behaving as a better solvent for the peptide.

DOPS supported the presence of MP1 up to the film collapse pressure. However, an LE character was not sufficient for MP1 to remain in the film at high surface pressures. DMPC films retained the peptide only up to 24–31 mN/m (depending on salt conditions), indicating that an increment in the lateral pressure and in-plane electrostatic repulsion of the cationic peptides destabilized the mixed film and induced expulsion of the peptide. A negatively charged lipid film is, thus, necessary to overcome the in-plane peptide repulsion and stabilizes the film.

The correlation observed between the final pressure of the collapse process and the π_e confirms that the high-pressure plateau observed in mixed monolayers corresponds to a peptide-enriched phase exclusion process since, above this pressure, no peptide can be further incorporated as a monomer into the lipid film. The insertion experiments show slightly higher values of π_e for almost all the MP1/lipid system studied compared with the pressure corresponding to the final peptide collapse. This is probably related to the formation of thicker peptide layers, as in the case of the adsorption to clean interfaces.

MP1 induced an increase in the surface pressure for the phase transition of DMPS and DPPC (Alvares et al., 2016) films and an enlargement of the area occupied by the LE phase, and induced the presence of this phase in the DPPS films. Similarly to what was found for DPPC/MP1, the thinner regions in the DMPS/MP1 mixture corresponded to the MP1-enriched phase in the LE phase, whilst the thicker regions were nearly pure lipids in the LC phase state. However, the exclusion of the peptide-enriched phase took place at much lower pressure than for the anionic monolayer (Table 2), evidencing an important role of the surface electrostatic stabilization of peptide at the interface.

To unravel the interesting effect of the lipid phases on the lipid-

peptide interaction, we determined the film thickness of the pure MP1, DMPS and DPPS films and DMPS/MP1 and DPPS/MP1 mixed films from reflectivity measures by BAM images. The monolayer of pure peptide was calculated to have a thickness of ~15 ± 3 Å. For pure lipid films, the thickness of the LE phase of DMPS was ~11 ± 3 Å, while the condensed phases of DMPS and DPPS were 20 ± 2 and 22 ± 2 Å, respectively. For DMPS/MP1 and DPPS/MP1 films, the thinner regions have a thickness similar to that of DMPS in the LE state. All these observations suggest that the thickness of MP1 in a transmembrane conformation matches the thickness of both PS in the LE phase, and this is one possible factor for the observed enrichment of MP1 in these regions.

The difference between the coexisting phases was also determined from the AFM images of DMPS/MP1 and DPPS/MP1 films, which is shown in Table S1 and illustrated in Fig. S3 (in Supplementary material). The difference between the LE and LC phases (~0.6 Å to DMPS/MP1 and ~0.8 Å to DPPS/MP1) was similar to that obtained from BAM images. In addition, the difference between the LC phase of DMPS/MP1 and DPPS/MP1 is consistent with a difference in height of 2 Å, calculated for these phases by the semi-empirical approach of Tanford (Tanford, 1972) and from BAM images.

5. Conclusion

Several independent techniques were used for assessing the influence of film thickness and phase state on negatively charged monolayers in the peptide/lipid interaction. All the techniques were consistent in showing a clear correlation between the peptide integration into the film and the occurrence of an anionic surface plus an LE phase. Using independent methods, we show a clear correlation of the surface pressure of expulsion of peptide (or lipid/peptide complex) in Langmuir films with the exclusion pressure obtained from penetration experiments, evidencing a robust behavior of the membrane. Additionally, a strong electrostatic attraction between MP1/PS film appears as an important membrane remodeling factor, inducing phase equilibrium displacement and thinning of the membrane. As was proposed by Bechinger (Bechinger, 2015), the disruption of the lipid packing and thinning of the membrane are important features for the mode of action of bioactive peptides.

The preferential adsorption of MP1 into PS films in the LE state induced the shift of the LE-LC transition pressure to higher values and also induced the presence of an LE phase, even when not occurring in the pure condensed lipid films (in the case of DPPS). In the last two decades, there has been considerable discussion of the importance of the presence of lipid domains in cell membranes either formed by sterol-enriched phases (Edidin, 2003) or LC phases (Grassmé et al., 2007) in coexistence with a disordered phase and its relation with cell functions (Rosetti et al., 2017). Ishii and collaborators (Ishii et al., 2005) show that the presence and integrity of these domains are necessary to maintain PS exposure in some type of cancer cells. The previous work of Alvares and collaborators (Alvares et al., 2017) gathered strong evidence about the synergies between PS and LC domains that enhance MP1 lytic activity in model bilayer systems. In this regard, the preferential partition of MP1 into the LE rather than the LC phase and the shifting of phase coexistence regions may be correlated with a greater insertion of MP1 into the LC domain boundary, which has been shown to be less organized (Kuzmin et al., 2005). In summary, the present work highlights the strong tendency of MP1 to be incorporated into PS membranes, which then regulates the membrane's physical properties. This interplay may be related with key regulation points in the binding and integration of this active peptide into membranes.

Acknowledgments

The authors acknowledge financial support from São Paulo Research Foundation − FAPESP (J.R.N. grants #2015/25619-9, #2011/11640-5, and 2011/51684-1, D.S.A has a Post-doctorate fellowship grant #2015/25620-7), Agencia Nacional de Promoción Científica y Tecnológica (ANPCyT, FONCyT − Argentina; grants PICT 2012-0344 and PICT 2014-1627), Consejo Nacional de Investigaciones Científicas y Técnicas (CONICET, PIP 2013-2015) and SECyT-Univ. Nacional de Córdoba. D.S.A also acknowledges FAPESP for PhD fellowships (grants #2012/08147-8 and BEPE-grants #2015/01508-3) that financed the research internship in the National University of Cordoba − Argentina. We would also like to thank UNESP and CAPES for their support in this research project. We also thank CEMETRO (UTN, Córdoba, Argentina) and Dr. C. Schurrer for their assistance in AFM experiments. J.R.N. is a researcher for Brazil's National Council for Scientific and Technological Development (CNPq). N.W. and M.L.F. are career researchers of CONICET (Argentina).

Appendix A. Supplementary data

Supplementary data associated with this article can be found, in the online version, at http://dx.doi.org/10.1016/j.chemphyslip.2017.08.001.

References

Alvares, D.S., Fanani, M.L., Ruggiero Neto, J., Wilke, N., 2016. The interfacial properties of the peptide Polybia-MP1 and its interaction with DPPC are modulated by lateral electrostatic attractions. Biochim. Biophys. Acta – Biomembr. 1858 (2), 393–402. http://dx.doi.org/10.1016/j.bbamem.2015.12.010.

Alvares, D.S., Neto, J.R., Ambroggio, E.E., 2017. Phosphatidylserine lipids and membrane order precisely regulate the activity of Polybia-MP1 peptide. Biochim. Biophys. Acta − Biomembr. http://dx.doi.org/10.1016/j.bbamem.2017.03.002.

Bechinger, B., 2015. The SMART model: soft membranes adapt and respond, also Transiently, in the presence of antimicrobial peptides. J. Pept. Sci. 21, 346–355. http://dx.doi.org/10.1002/psc.2729.

Birdi, K.S., 2006. Self-Assembly Monolayer Structures of Lipids and Macromolecules at Interfaces. Springer, US.

Boisselier, É., Calvez, P., Demers, É., Cantin, L., Salesse, C., 2012. Influence of the physical state of phospholipid monolayers on protein binding. Langmuir 28, 9680–9688. http://dx.doi.org/10.1021/la301135z.

Boisselier, É., Demers, É., Cantin, L., Salesse, C., 2017. How to gather useful and valuable information from protein binding measurements using Langmuir lipid monolayers. Adv. Colloid Interface Sci. 1–17. http://dx.doi.org/10.1016/j.cis.2017.03.004.

Bouffioux, O., Berquand, A., Eeman, M., Paquot, M., Dufrêne, Y.F., Brasseur, R., Deleu, M., 2007. Molecular organization of surfactin-phospholipid monolayers: effect of phospholipid chain length and polar head. Biochim. Biophys. Acta − Biomembr. 1768, 1758–1768.

Bougis, P., Rochat, H., Piéroni, G., Verger, R., 1981. Penetration of phospholipid monolayers by cardiotoxins. Biochemistry 20, 4915–4920.

Brockman, H.L., 1999. Lipid monolayers: why use half a membrane interactions? to characterize. Curr. Opin. Struct. Biol. 9, 438–443.

Bueno Leite, N., Aufderhorst-Roberts, A., Palma, M.S., Connell, S.D., Ruggiero Neto, J., Beales, P.A., 2015. PE and PS lipids synergistically enhance membrane poration by a peptide with anticancer properties. Biophys. J. 109, 936–947. http://dx.doi.org/10.1016/j.bpj.2015.07.033.

Chen, X., Huang, Z., Hua, W., Castada, H., Allen, H.C., 2010. Reorganization and caging of DPPC, DPPE, DPPG, and DPPS monolayers caused by dimethylsulfoxide observed using brewster angle microscopy. Langmuir 26, 18902–18908.

Daear, W., Mahadeo, M., Prenner, E.J., 2017. Applications of Brewster angle microscopy from biological materials to biological systems. Biochim. Biophys. Acta − Biomembr. 1859, 1749–1766. http://dx.doi.org/10.1016/j.bbamem.2017.06.016.

De Tullio, L., Maggio, B., Fanani, M.L., 2008. Sphingomyelinase acts by an area-activated mechanism on the liquid-expanded phase of sphingomyelin monolayers. J. Lipid Res. 49, 2347–2355. http://dx.doi.org/10.1194/jlr.M800127-JLR200.

Devaux, P.F., 1992. Protein involvement in transmembrane lipid asymmetry. Annu. Rev. Biophys. Biomol. Struct. 21, 417–439.

Dos Santos Cabrera, M.P., Arcisio-Miranda, M., Gorjão, R., Leite, N.B., De Souza, B.M., Curi, R., Procopio, J., Ruggiero Neto, J., Palma, M.S., 2012. Influence of the bilayer composition on the binding and membrane disrupting effect of polybia-MP1, an antimicrobial mastoparan peptide with leukemic T-lymphocyte cell selectivity. Biochemistry 51, 4898–4908. http://dx.doi.org/10.1021/bi201608d.

Dyck, M., Kerth, A., Blume, A., Losche, M., 2006. Interaction of the neurotransmitter, neuropeptide Y, with phospholipid membranes: infrared spectroscopic characterization at the air/water interface. J. Phys. Chem. B 110, 22152–22159. http://dx.doi.org/10.1021/jp062537q.

Edidin, M., 2003. The state of lipid rafts: from model membranes to cells. Annu. Rev. Biophys. Biomol. Struct. 32, 257–283. http://dx.doi.org/10.1146/annurev.biophys.32.110601.142439.

Fadok, V.A., Voelker, D.R., Campbell, P.A., Cohen, J.J., Bratton, D.L., Henson, P.M., 1992.

Exposure of phosphatidylserine on the surface of apoptotic lymphocytes triggers specific recognition and removal by macrophages. J. Immunol. 148, 2207–2216.
Fadok, V.A., Bratton, D.L., Frasch, S.C., Warner, M.L., Henson, P.M., 1998. The role of phosphatidylserine in recognition of apoptotic cells by phagocytes. Cell Death Differ. 5, 551–562.
Fanani, M.L., Hartel, S., Maggio, B., De Tullio, L., Jara, J., Olmos, F., Oliveira, R.G., 2010. The action of sphingomyelinase in lipid monolayers as revealed by microscopic image analysis. Biochim. Biophys. Acta − Biomembr. 1798, 1309–1323. http://dx.doi.org/10.1016/j.bbamem.2010.01.001.
Fezoua-Boubegtiten, Z., Desbat, B., Brisson, A., Lecomte, S., 2010. Determination of molecular groups involved in the interaction of annexin A5 with lipid membrane models at the air-water interface. Biochim. Biophys. Acta − Biomembr. 1798, 1204–1211. http://dx.doi.org/10.1016/j.bbamem.2010.03.014.
Fidelio, G.D., Maggio, B., Cumar, F.A., 1986. Stability and penetration of soluble and membrane proteins in interfaces. An. Asoc. Quim. Argent. 74, 801–813.
Gaines, G.L., 1966. Insoluble monolayers at liquid-gas interfaces. Interscience Publishers, New York. http://dx.doi.org/10.1016/0021-9797(66)90041-5.
Grassmé, H., Riethmüller, J., Gulbins, E., 2007. Biological aspects of ceramide-enriched membrane domains. Prog. Lipid Res. 46, 161–170. http://dx.doi.org/10.1016/j.plipres.2007.03.002.
Gudmand, M., Rocha, S., Hatzakis, N.S., Peneva, K., Müllen, K., Stamou, D., Uji-I, H., Hofkens, J., Bjørnholm, T., Heimburg, T., 2010. Influence of lipid heterogeneity and phase behavior on phospholipase A 2 action at the single molecule level. Biophys. J. 98, 1873–1882. http://dx.doi.org/10.1016/j.bpj.2010.01.035.
Heimburg, T., 2007. Thermal Biophysics of Membranes. WILEY-VCH Verlag GmbH & Co. KGaA, Germany.
Ishii, H., Mori, T., Shiratsuchi, A., Nakai, Y., Shimada, Y., Ohno-Iwashita, Y., Nakanishi, Y., 2005. Distinct localization of lipid rafts and externalized phosphatidylserine at the surface of apoptotic cells. Biochem. Biophys. Res. Commun. 327, 94–99.
Kienle, D.F., De Souza, J.V., Watkins, E.B., Kuhl, T.L., 2014. Thickness and refractive index of DPPC and DPPE monolayers by multiple-beam interferometry. Anal. Bioanal. Chem. 406, 4725–4733. http://dx.doi.org/10.1007/s00216-014-7866-9.
Kuzmin, P.I., Akimov, S.A., Chizmadzhev, Y.A., Zimmerberg, J., Cohen, F.S., 2005. Line tension and interaction energies of membrane rafts calculated from lipid splay and tilt. Biophys. J. 88, 1120–1133. http://dx.doi.org/10.1529/biophysj.104.048223.
Maget-Dana, R., Ptak, M., 1995. Interactions of surfactin with membrane models. Biophys. J. 68, 1937–1943.
Maget-Dana, R., 1999. The monolayer technique: a potent tool for studying the interfacial properties of antimicrobial and membrane-lytic peptides and their interactions with lipid membranes. Biochimica et Biophysica Acta 1462, 109–140. http://dx.doi.org/10.1016/S0005-2736(99)00203-5.
Mangiarotti, A., Caruso, B., Wilke, N., 2014. Phase coexistence in films composed of DLPC and DPPC: A comparison between different model membrane systems. Biochim. Biophys. Acta − Biomembr. 1838, 1823–1831. http://dx.doi.org/10.1016/j.bbamem.2014.02.012.
Marsh, D., 1996. Lateral pressure in membranes. Biochim. Biophys. Acta − Rev. Biomembr. 1286, 183–223. http://dx.doi.org/10.1016/S0304-4157(96)00009-3.
Mottola, M., Wilke, N., Benedini, L., Oliveira, R.G.R.G., Fanani, M.L., 2013. Ascorbyl palmitate interaction with phospholipid monolayers: electrostatic and rheological preponderancy. Biochim. Biophys. Acta − Biomembr. 1828, 2496–2505. http://dx.doi.org/10.1016/j.bbamem.2013.06.016.
Mottola, M., Vico, R.V., Villanueva, M.E., Fanani, M.L., 2015. Alkyl esters of l-ascorbic acid: stability, surface behaviour and interaction with phospholipid monolayers. J. Colloid Interface Sci. 457, 232–242. http://dx.doi.org/10.1016/j.jcis.2015.07.014.
Nobre, T.M., Pavinatto, F.J., Caseli, L., Barros-Timmons, A., Dynarowicz-Łatka, P., Oliveira, O.N., 2015. Interactions of bioactive molecules & nanomaterials with Langmuir monolayers as cell membrane models. Thin Solid Films 593, 158–188. http://dx.doi.org/10.1016/j.tsf.2015.09.047.
Pedrera, L., Fanani, M.L., Ros, U., Lanio, M.E., Maggio, B., Álvarez, C., 2014. Sticholysin I-membrane interaction: an interplay between the presence of sphingomyelin and membrane fluidity. Biochim. Biophys. Acta − Biomembr. 1838, 1752–1759. http://dx.doi.org/10.1016/j.bbamem.2014.03.011.
Polozov, I.V., Polozova, a. I., Molotkovsky, J.G., Epand, R.M., 1997. Amphipathic peptide affects the lateral domain organization of lipid bilayers. Biochim. Biophys. Acta − Biomembr. 1328, 125–139.
Pusterla, J.M., Malfatti-Gasperini, A. a., Puentes-Martinez, X.E., Cavalcanti, L.P., Oliveira, R.G., 2017. Refractive index and thickness determination in Langmuir monolayers of myelin lipids. Biochim. Biophys. Acta − Biomembr. 1859, 924–930. http://dx.doi.org/10.1016/j.bbamem.2017.02.005.
Riedl, S., Rinner, B., Asslaber, M., Schaider, H., Walzer, S., Novak, A., Lohner, K., Zweytick, D., 2011. In search of a novel target − Phosphatidylserine exposed by non-apoptotic tumor cells and metastases of malignancies with poor treatment efficacy. Biochim. Biophys. Acta − Biomembr. 1808, 2638–2645.
Rosetti, C.M., Mangiarotti, A., Wilke, N., 2017. Sizes of lipid domains: what do we know from artificial lipid membranes? What are the possible shared features with membrane rafts in cells? Biochim. Biophys. Acta − Biomembr. 1859, 789–802. http://dx.doi.org/10.1016/j.bbamem.2017.01.030.
Souza, B.M., Mendes, M.A., Santos, L.D., Marques, M.R., César, L.M., Almeida, R.N., Pagnocca, F.C., Konno, K., Palma, M.S., 2005. Structural and functional characterization of two novel peptide toxins isolated from the venom of the social wasp Polybia paulista. Peptides 26, 2157–2164. http://dx.doi.org/10.1016/j.peptides.2005.04.026.
Tanford, C., 1972. Micelle shape and size. J. Phys. Chem. 76, 3020–3024.
Tocanne, J.F., Teissie, J., 1990. Ionization of phospholipids and phospholipid-supported interfacial lateral diffusion of protons in membrane model systems. Biochim. Biophys. Acta − Rev. Biomembr. 1031, 111–142. http://dx.doi.org/10.1016/0304-4157(90)90005-W.
Tsui, F.C., Ojcius, D.M., Hubbell, W.L., 1986. The intrinsic pKa values for phosphatidylserine and phosphatidylethanolamine in phosphotidylcholine host bilayers. Biophys. J. 49, 459–468.
Utsugi, T., Schroit, A.J., Connor, J., Bucana, C., Fidler, I.J., 1991. Elevated Expression of Phosphatidylserine in the Outer Membrane Leaflet of Human Tumor Cells and Recognition by Activated Human Blood Monocytes Advances in Brief Elevated Expression of Phosphatidylserine in the Outer Membrane Leaflet of Human Tumor Cells. pp. 3062–3066.
Vega Mercado, F., Maggio, B., Wilke, N., 2011. Phase diagram of mixed monolayers of stearic acid and dimyristoylphosphatidylcholine. Effect of the acid ionization. Chem. Phys. Lipids 164, 386–392. http://dx.doi.org/10.1016/j.chemphyslip.2011.05.004.
Vollhardt, D., Fainerman, V.B., 2010. Characterisation of phase transition in adsorbed monolayers at the air/water interface. Adv. Colloid Interface Sci. 154, 1–19. http://dx.doi.org/10.1016/j.cis.2010.01.003.
Wang, K., Zhang, B., Zhang, W., Yan, J., Li, J., Wang, R., 2008. Antitumor effects, cell selectivity and structure-activity relationship of a novel antimicrobial peptide polybia-MPI. Peptides 29, 963–968. http://dx.doi.org/10.1016/j.peptides.2008.01.015.
Wang, K., Yan, J., Zhang, B., Song, J., Jia, P., Wang, R., 2009. Novel mode of action of polybia-MPI, a novel antimicrobial peptide, in multi-drug resistant leukemic cells. Cancer Lett. 278, 65–72. http://dx.doi.org/10.1016/j.canlet.2008.12.027.
Wilke, N., 2014. Lipid monolayers at the Air–Water interface: a tool for understanding electrostatic interactions and rheology in biomembranes. Advances in Planar Lipid Bilayers and Liposomes. Elsevier Inc.pp. 51–81.
Zulueta Díaz, Y. de las M., Fanani, M.L., 2017. Crossregulation between the insertion of Hexadecylphosphocholine (miltefosine) into lipid membranes and their rheology and lateral structure. Biochim. Biophys. Acta − Biomembr. 1859, 1891–1899. http://dx.doi.org/10.1016/j.bbamem.2017.06.008.
Zulueta Diaz, Y. de las M., Mottola, M., Vico, R.V., Wilke, N., Fanani, M.L., 2016. The rheological properties of lipid monolayers modulate the incorporation of l – ascorbic acid alkyl esters. Langmuir 32, 587–595. http://dx.doi.org/10.1021/acs.langmuir.5b04175.